LOCK-IN THERMOGRAPHY ON CRYSTALLINE SILICON ON GLASS (CSG) THIN FILM MODULES: INFLUENCE OF PELTIER CONTRIBUTIONS

H. Straube, O. Breitenstein, J.-M. Wagner
Max Planck Institute of Microstructure Physics
Weinberg 2, D-06120 Halle, Germany

ABSTRACT: In this contribution we describe electro-thermal modeling of a CSG thin film silicon solar cell under pulsed bias. The model is aimed at extracting cell parameters locally through comparison with lock-in thermography (LIT) results over a wide voltage range. The cell is divided into a number of volume elements for Spice electronics simulations. The results are imaged and convoluted with the appropriate point spread function for a highly heat conductive silicon layer on a thick glass substrate. Peltier effects must be taken into account since p and n type contact holes are separated from each other and are resolved in the thermograms. Values for the test module's area diode saturation currents, nonlinear edge shunts, and series resistance resulting from a manual fit of experimental and simulated thermograms are presented.
Keywords: Characterization, Polycrystalline Si-Films, Lock-in Thermography, Peltier Effect

1 INTRODUCTION

Dark lock-in thermography (DLIT) has proven to be a successful tool to quantify loss mechanisms in mono- and multi-crystalline solar cells [1]. It gives images of the local power distribution (mW/m²) in the sample. The interpretation of thermograms of thin film modules such as CSG [2], however, is more difficult than that of standard cells, due to the more complex patterning and particularly due to strong Peltier contributions at the contacts.

This was seen while studying edge recombination heating at the laser grooves separating cells. Two observations were made. Firstly, at low voltages, contact holes close to these edges were found to present a negative DLIT signal. This means that here the Peltier cooling is locally stronger than contributions from heat dissipation at the junction, sheet and contact resistances. Since the Peltier heat absorbed at the contacts is released on crossing the junction, this effect can strongly affect quantitative evaluation of localized shunting phenomena. Secondly, the cell edges appear brighter than the rest of the cell at low cell current (around maximum power point voltage). At higher currents, the contrast becomes inversed and the edges get less intense than the cell area. A correct model must describe this contrast reversal appropriately.

To build such a model, the *Peltier coefficients* were measured on test structures of the thin film material (section 2). Since the current distribution in a cell is not homogenous a *circuit model of the cell* was developed (for the PSpice circuit simulator, section 3.2). The results of the electrical simulation were then translated into a map of heat generation (local power dissipation and Peltier heat). *Convolution* of this heat generation map with the thermal point spread function gives the temperature modulation signal measured in DLIT (section 3.3). Finally, comparison of the measured data to the calculated DLIT signal allows meaningful *conclusions about cell parameters* (section 4).

1.1 CSG module layout

Before a detailed description of the measurements and simulations, a few words about the CSG thin film module structure are indicated.

Each module consists of 6 mm broad stripes of 1.5 µm thick silicon on glass, separated by 25 µm wide grooves. These stripes are the individual cells. The light enters the silicon through the glass superstrate side. From the glass side, it is an n^+-p-p^+ structure. The cells are interconnected by 0.5 mm wide aluminum pads that span two cells each and are arranged in an interdigitated pattern (see Figure 1). Each contact pad has a number of contact holes reaching to the n^+ layer in the upper cell or connecting the p^+ layer in the lower cell, respectively. In the modules used in this study, each contact pad had 14 n and 14 p contact holes. For details about this contacting scheme and its benefits, see [3].

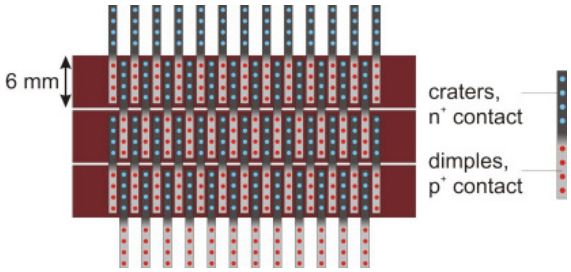

Figure 1: CSG module layout with three silicon cell stripes and corresponding interconnectors. Only 2×4 of 2×14 contact holes per pad are drawn.

2 MEASUREMENT OF THE PELTIER COEFFICIENT

2.1 Basics

In a recent contribution we described how to measure the Peltier coefficient of semiconductor material thermographically [4]. The basic argument is as follows:

In the case of silicon on glass the -45° signal S from the lock-in process is directly proportional to the heating density Q (blurred with the point spread function).

In a purely resistive sample under isothermal conditions Joule (S^J) and Peltier (S^P) heating signal (corresponding to the heating terms Q^J, Q^P) in every point are even or odd functions of the bias, respectively. Therefore, adding and subtracting signals obtained at positive (S^+) and negative bias (S^-) gives separate images proportional to Joule and Peltier heating contributions:

$$S^J = (S^+ + S^-)/2$$
$$S^P = (S^+ - S^-)/2 \quad (1)$$

For a homogenous current flow, straightforward calculations give an expression for the Peltier coefficient Π that does not depend on the ratio of heating density and signal (hence no calibration is needed):

$$\Pi = -U \frac{\int_{A-d}^{A+d} S^P dx}{\int_{A-d}^{B+d} S^J dx} = +U \frac{\int_{B-d}^{B+d} S^P dx}{\int_{A-d}^{B+d} S^J dx}, \qquad (2)$$

where A and B are the (metallic) contacts, where the current enters and leaves the semiconductor. U is the voltage applied between them (A positive). The integration has to be extended a distance d over the actual contacts in order to collect the whole signal blurred by the point spread function of the system.

2.2 Peltier coefficients in CSG

CSG Solar routinely manufactures series resistance test structures which differ from the regular structure (see Figure 1) only by that *every* contact hole is either dimple (to p^+) or crater (to n^+). In such a structure the current never crosses any p-n junction throughout the module. These structures are thus purely resistive and the procedure for measuring the Peltier coefficient Π outlined above can be applied. The resistive test structure used here is part of the same batch as the actual module that is modeled.

Typical images are shown in Figure 2. Note that at every contact pad there is a homogenous current flow to the left and to the right such that the signals under each pad are twice as high as supposed for (2). The radius d in (2) is about 0.2 mm.

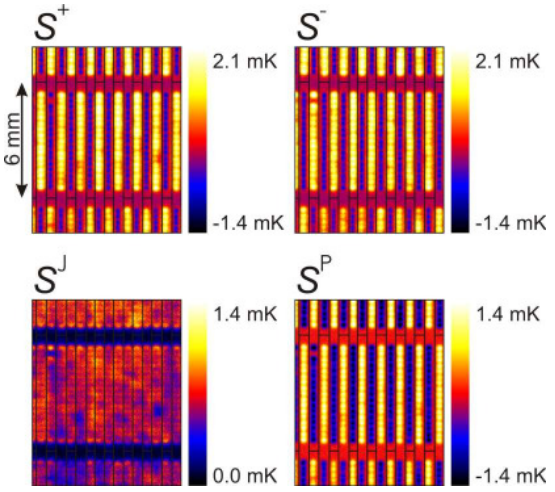

Figure 2: Measured signals S^+, S^- and corresponding Joule S^J and Peltier S^P contributions calculated from (1) in the p region of the CSG resistive test structure. Contact pad locations are marked with solid lines.

The Peltier coefficient Π is found to be +(90±5) mV for the p^+ region and –(90±5) mV for the n^+ region (U=200 mV for p^+, U=100 mV for n^+, at approximately short circuit current equivalent). The physical meaning and origin of these values is detailed in [4]. Following the procedures outlined in [4] dopant concentrations of 4×10^{19} cm^{-3} and 2×10^{19} cm^{-3} for n^+ and p^+, respectively, are estimated.

Halving the voltages gives the same results for the Peltier coefficients, which confirms the symmetries used to derive (2).

2.3 Applicability check for CSG

The approach of section 2.1/2.2 requires isothermal conditions over the sample surface. In the case of thin film cells on a thick glass substrate, these cannot be imposed by an external temperature control. However, it can be shown that (2) is still valid by calculating an upper bound to the additional thermoelectric heating terms not considered above. This upper bound is calculated below.

In the lock-in process, the temperature at every point can be described by an oscillating contribution and a spatially varying mean temperature $\overline{T}(\mathbf{r}) = T_0 + T_\Delta(\mathbf{r})$. Only the oscillating contribution is detected in the lock-in measurement. The stationary temperature inhomogeneities $T_\Delta(\mathbf{r})$ occur only because no temperature control can be applied for a (thermally thick) substrate and give rise to additional thermoelectric contributions. $T_\Delta(\mathbf{r})$ can be calculated by solving the stationary heat conduction equation, assuming only half the heating power Q, since in the lock-in process the current is flowing only half of the time (κ heat conductivity):

$$\kappa \Delta \overline{T} = Q/2 \,. \qquad (3)$$

It is known that both the highly doped p^+ and n^+ layers have Peltier coefficients less than 100 mV [4]. The Joule heating sheet resistance is fairly homogenous, and it need not be considered here. The temperature profile of a disk of homogenous Peltier heating (disregarding for the time being any further effects) can be calculated by solving (3) numerically and is shown in Figure 3. It was assumed that each contact hole carries the same current as in an actual module under short circuit conditions (≈ 22 mA/cm^2 or ≈ 50 µA per contact hole).

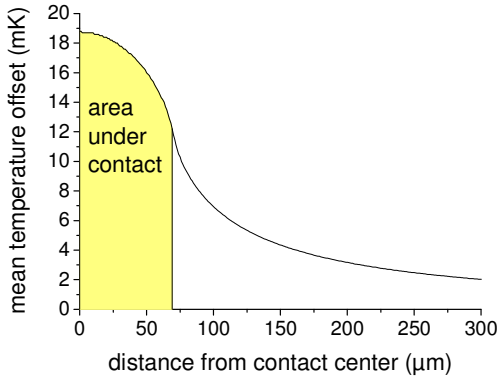

Figure 3: Mean temperature inhomogeneity T_Δ around a contact hole (heating), assuming a Peltier coefficient of 100 mV and a current of 50 µA.

The systematic errors caused by this temperature distribution are due to additional thermoelectric effects. In that case the heating power Q [the source term of the oscillatory part of the heat conduction equation (4)] is [5]:

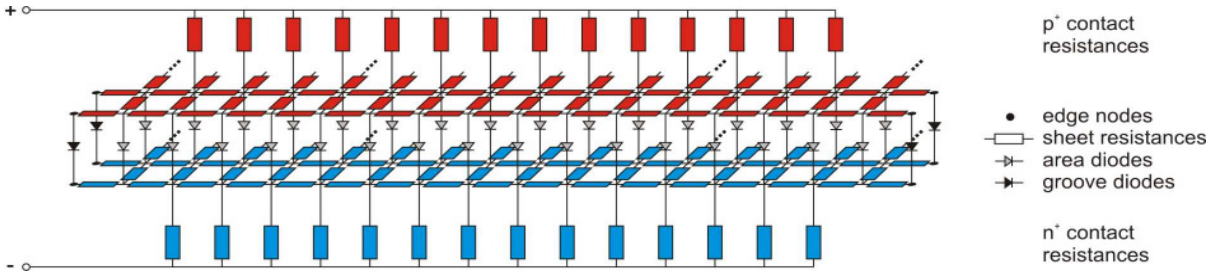

Figure 4: Spice model for a 1 mm wide portion of a CSG cell. In the first line, the n^+ region (blue) is connected to the next cell of the module by 14 contact holes (below). In the second line, 14 contact holes (above) contact the p^+ region (red) to the previous cell. The elementary diodes, distributed according to the location of the contact holes, are interconnected by the sheet resistivity in the p^+ and n^+ layers.

$$\begin{aligned} Q(\mathbf{r}) = {} & \rho(\mathbf{r})\mathbf{j}(\mathbf{r})^2 \\ & - \mathbf{j}(\mathbf{r}) \cdot T_0 \nabla \alpha(\mathbf{r},T) \\ & - \mathbf{j}(\mathbf{r}) \cdot T_\Delta(\mathbf{r}) \nabla \alpha(\mathbf{r},T) \\ & - \mathbf{j}(\mathbf{r}) \cdot \tau(\mathbf{r}) \nabla T_\Delta(\mathbf{r}), \end{aligned}$$

where τ is the Thomson coefficient, and the temperature dependence of α is taken to be explicit. Please note the Thomson relations $\tau = T \cdot \partial\alpha/\partial T$ and $\Pi = \alpha T$. The first two terms $\rho\mathbf{j}^2$ (Joule heating) and $-\mathbf{j}T_0\nabla\alpha = -\mathbf{j}\nabla\Pi_0$ (isothermal Peltier heat transport) are the ones already discussed in section 2.1.

In the test structure the Joule heating term is equally strong in the whole structure:

$$\rho\mathbf{j}^2 = 1000\,\Omega/\mathrm{sq} \times (330\,\mu\mathrm{A}/6\mathrm{mm})^2 = 3\,\mathrm{W/m^2}$$

The Peltier term only appears directly under the contacts as does the third term ($\nabla\alpha$ is a step function at the metal-semiconductor interface)

$$\begin{aligned} -\frac{I}{A} T_0 \alpha &= -\frac{660\,\mu\mathrm{A}/14}{\pi(70\,\mu\mathrm{m})^2} \times 300\,\mathrm{K} \times (0.1\,\mathrm{V}/300\,\mathrm{K}) \\ &= -306\,\mathrm{W/m^2} \\ -\frac{I}{A} T_\Delta \alpha &= -\frac{660\,\mu\mathrm{A}/14}{\pi(70\,\mu\mathrm{m})^2} \times 20\,\mathrm{mK} \times (0.1\,\mathrm{V}/300\,\mathrm{K}) \\ &= -0.02\,\mathrm{mW/m^2} \end{aligned}$$

The fourth term, the Thomson effect, is strongest at the highest temperature gradient which is at the contact hole's circumference.

$$\begin{aligned} -\mathbf{j}\tau\nabla T_\Delta &= -\frac{660\,\mu\mathrm{A}/14}{2\pi(70\,\mu\mathrm{m})} \times 0.2\,\mathrm{mV/K} \times 400\,\mathrm{K/m} \\ &= -0.0086\,\mathrm{W/m^2} \end{aligned}$$

Thus, both additional terms appearing since the surface temperature cannot be forced to a constant value (i.e. $T_\Delta(\mathbf{r}) \neq 0$), are small compared to the terms considered in section 2.1. Hence, equation (2) can be used to determine the Peltier coefficient.

3 SIMULATION PROCEDURE

3.1 Overview

A single cell consisting of a periodic arrangement of contact pads was divided into diodes and resistors suitable for calculations with Spice (PSpice version 9.2). The Spice simulation output file was then parsed for the individual diodes and resistors whose heat dissipation and Peltier type heat transport are copied into a map of the local heating density Q, that can have negative values because of the Peltier effect.

This map can then be convoluted with the appropriate point spread function (PSF) to give the simulated LIT images that can be compared to the experimental images.

Realistic values for the diode saturation currents are extracted by adjusting the model parameters to the data at high and low currents.

3.2 Spice model

The area under each contact hole is modeled by one diode and these diodes are interconnected by resistors corresponding to the sheet resistivity (Ω/sq) of the p^+ and n^+ regions, respectively. Additionally, two area diodes have been introduced to the regions without contact holes near the cell edges in order to better assess series resistance losses there. Lock-in thermograms of CSG modules show a pronounced signal at the laser cut lines (grooves) between the cells. This signal is not ohmic and was modeled as an extra diode with elevated saturation current. The model components for a small part of a single cell are shown in Figure 4. For every diode in the Figure, a n=1 diode and a n=2 recombination diode are assumed.

For comparison with experiment a region of the module without any shunts was used so that no parallel resistors had to be introduced in the model. The effects of shunting in a CSG module are described elsewhere [3].

The result of the Spice simulation is a set of currents I and voltages U for every simulated resistor and diode of which the corresponding areas A in the image plane are known. The current information can be used to draw a *map of the Peltier power distribution* which is given by $Q^\mathrm{P} = -\nabla \cdot (\mathbf{j}\Pi)$. This is easy to evaluate at the contact holes because there Π is just a step function between the (negligibly small) Peltier coefficient of the aluminum and the silicon p^+ or n^+ layers, respectively. With the known current through the contact resistors the Peltier heat density is given by

$$\mathrm{Al\ to\ p^+}: \quad Q^\mathrm{P} = \left(I / A_\mathrm{contact}\right) \times \left(-\Pi_{p+}\right),$$

$$\mathrm{n^+\ to\ Al}: \quad Q^\mathrm{P} = \left(I / A_\mathrm{contact}\right) \times \Pi_{n+}.$$

Both contributions are negative under forward bias.

Due to the low diffusion length in a thin film cell, minority carriers cannot move appreciably in the image plane and the actual shape of the Peltier coefficient across the p-n junction is insignificant. Therefore it holds that the overall Peltier heat contribution is just:

$$\mathrm{p^+\ to\ n^+}: \quad Q^\mathrm{P} = \left(I / A_\mathrm{contact}\right) \times \left(\Pi_{p+} - \Pi_{n+}\right).$$

This contribution is always positive and cancels the cooling from the contacts. Note that the energy-conserving

Peltier heat transport has no effect on the performance of the module, but has to be considered when evaluating lock-in thermograms.

The *map of power dissipation* $Q^J = \mathbf{j} \cdot \mathbf{E}$ can be drawn in a straightforward manner from the current-voltage information for each element of the Spice simulation output,

$Q^J = |IU| / A$.

3.3 Convolution with the point spread function (PSF)

Trying to convolve the power maps Q^J, Q^P, Q^J+Q^P generated through the Spice simulation we noted that both the model of heat wave propagation through a thermally thin and a thermally thick medium [1] are not valid for the silicon on glass structure. Instead, both the heat propagation through the 1.5 µm thick silicon layer and through the thick glass superstrate have to be taken into account.

The problem is thus that of solving the three-dimensional heat conduction equation

$$\Delta T - \frac{1}{D}\frac{\partial T}{\partial t} = Q \qquad (4)$$

with the boundary condition of two-dimensional heat flow in the silicon layer on the surface

$$\Delta_2 T - \frac{\kappa}{d\kappa_f}\frac{\partial T}{\partial z} - \frac{1}{D_f}\frac{\partial T}{\partial t} = 0, \qquad (5)$$

where Δ and Δ_2 are the three and two-dimensional Laplace operators, respectively, D denotes the diffusivity and κ the heat conductivity. The index f is used for film quantities. An analytical solution to these equations is possible and will be detailed in an upcoming publication [6]. The solution for the present case in comparison with the limiting cases of heat wave propagation through thermally thin and thick media is shown in Figure 5.

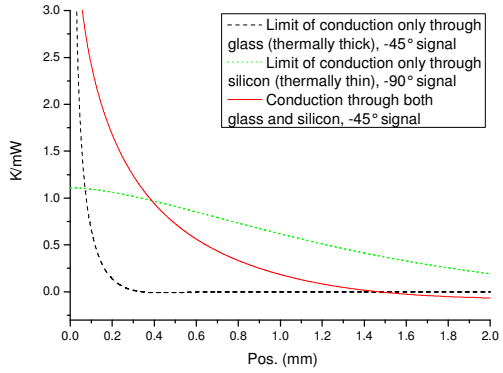

Figure 5: Point spread functions for the case of silicon on glass in comparison with the limiting cases of heat wave propagation through thermally thin and thick media (maximum intensity single phase signal, -90° for thermally thick, -45° for the other cases)

Unfortunately, there is a problem with the convolution at the grooves that separate the individual cells from each other, since at those lines the (highly heat conductive) silicon film is interrupted and the boundary condition (5) no longer holds. Here, we decided to avoid this difficulty by assuming periodic continuation of the power distribution over the grooves in the simulation and providing an approximately periodic continuation in the experiment through the neighboring cells in the module. In this way the heat flux across the groove is minimized.

4 FIT PROCEDURE AND RESULTS

Realistic values for the cell parameters can be extracted by comparing images (Figure 6) and linescans (Figure 7) from experiment and simulation. Both simulated and experimental images can be scaled in mW/m² with only the known overall current/voltage values, i.e. an arbitrary scaling factor is not necessary.

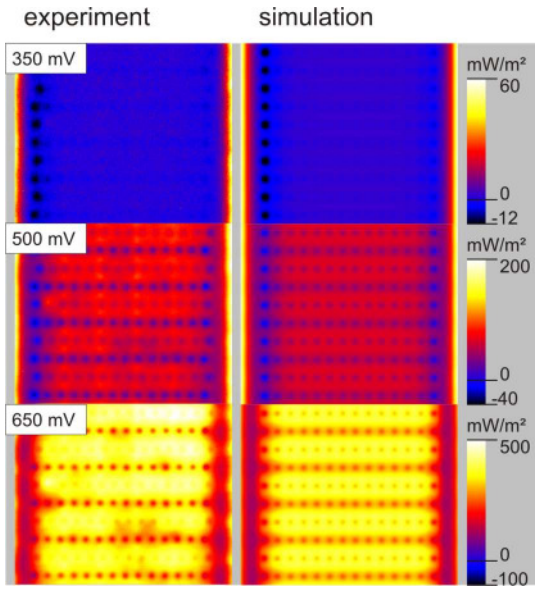

Figure 6: Maps of heating power density from experiment (left) and simulation (right) at low, medium and high voltages for the values cited in Table I. The maximum power point was at approx. 400 mV. Note the contrast reversal between grooves and area for low and high currents.

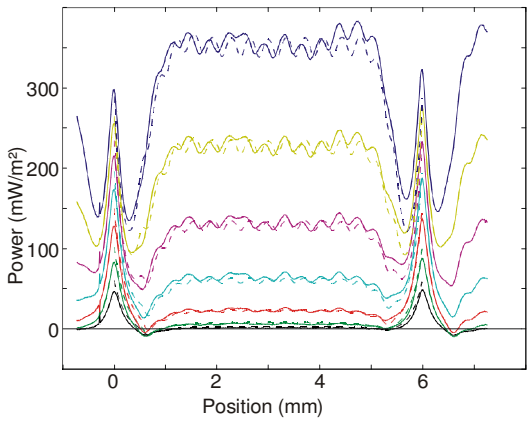

Figure 7: Horizontal linescans of experimental (solid lines) and simulated thermograms (dashed lines) averaged across 10 cell pads (5 mm). Voltages range from 350 mV (black) to 650 mV (blue) in steps of 50 mV.

The geometry parameters (number of contact holes, pad width, etc.) are easily accessible and their error is negligible. The Peltier coefficient was determined on a test structure in the same sample batch (see section 2.2) and was assumed to be the same for the module. Both the

contact hole and sheet resistances used in the simulation were measured on another full module of the same batch. This measurement could not be done on the same module since it involves cutting the contact pads.

At the center of the cell the effect of the grooves is low and the area-averaged Peltier effects cancel as they do in a standard solar cell. Therefore, with the signal $Q=UI$ in the center of the cell, the area current densities J_{01}, J_{02} and the sum of the resistances could be determined.

The ratio of p^+ to n^+ sheet resistance can be determined by looking at the linescans perpendicular to the pads. As can be seen in Figure 6, the lower series resistance in the n^+ region causes more heat to be dissipated below the p^+ type contacts.

Finally, the groove diodes can be adjusted via the asymmetry of the linescans in Figure 7. The left groove draws significantly more current than the right one as can be seen in the 350 mV part of Figure 6, where the current flows dominantly from the left contact holes (Peltier cooling at the contacts) to the left cell edge. (These differences in the currents through the inner and outer contact holes get less pronounced at higher voltages. Therefore the assumption of equal currents through every contact hole in the estimation of thermoelectric effects in section 2.3 is also valid for modules.) Unfortunately, the ratio of current drawn by the left cell edge to that drawn by the right cell edge can only be determined very inaccurately because the groove signals of neighboring cells cannot be distinguished, it is between 0.01 and 0.1. Here a ratio of about 0.05 was assumed. Accordingly, the absolute values of the line groove currents J_{01}, J_{02} given in A per cm groove length, are only known to their order of magnitude.

The parameters of this (manual) best fit simulation are shown in Table I. Values in italic were not varied as they are known from other modules (Peltier coefficients and contact hole resistances) or are simple geometry parameters.

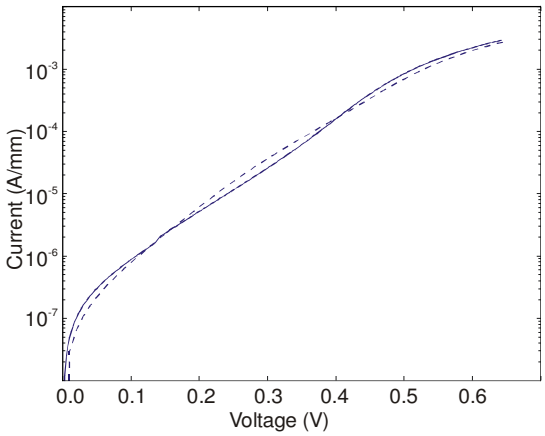

Figure 8: Experimental (solid lines) and simulated (dashed lines) current-voltage characteristic normalized to 1 mm length of a (6 mm wide) cell stripe.

Table I: Simulation parameters

	Value	± (approx.)
p hole contact resistance	49 Ω	5 % (diff. module)
n hole contact resistance	154 Ω	5 % (diff. module)
p sheet resistance	1.8 kΩ	10 %
n sheet resistance	1.1 kΩ	10 %
area J_{01}	$7.4\cdot10^{-11}$ A/cm^2	10 %
area J_{02}	$9.7\cdot10^{-11}$ A/cm^2	10 %
left groove J_{01}	$4.75\cdot10^{-9}$ A/cm	(see text)
left groove J_{02}	$7.60\cdot10^{-7}$ A/cm	(see text)
right groove J_{01}	$2.50\cdot10^{-10}$ A/cm	(see text)
right groove J_{02}	$4.00\cdot10^{-8}$ A/cm	(see text)
p Peltier coefficient	90 mV	5 % (test struct.)
n Peltier coefficient	–90 mV	5 % (test struct.)
contact holes per pad	14	
pad width	0.5 mm	
distance groove-groove	6 mm	
dist. between contact holes	0.36 mm	
contact hole radius	70 µm	

Note that the contact holes are always colder than their environment because of the Peltier cooling there (in spite of their contact resistances, Figure 6). In the cell center the cooling at the contacts and the heating at the diodes is less than half a millimeter (one pad width) separated which results in only a slight oscillation in the linescans. At the edges the distance of the outer contact holes to the cell grooves is much longer and the contrast between Peltier cooling at the contact holes and heating at the diodes is plainly visible (Figure 7).

Figure 8 shows a comparison of the *I-V* characteristics of the whole experimental eight cell mini-module to the *I-V* characteristics of the simulated cell resulting from the values of Table I. Both curves are normalized to a 1 mm long portion of a cell, no further correction factors were applied.

5 CONCLUSION AND OUTLOOK

In this contribution we showed how to fully understand the behavior of a CSG structure in DLIT over a wide voltage range. A strong Peltier contribution is observed and included in the thermal simulation, since n and p contact holes are resolved. A shunt-free region was modeled in Spice, the results were mapped in an image of local power dissipation and convoluted with the point spread function of a highly heat conductive layer on a glass substrate. Edge (groove) and area diode properties were separately observed and could be quantified through a fit of the simulations to the experimental data. Direct *I-V* curve measurement would only give a mixture of both effects.

The strength of this groove shunting is different for both edges of the cell (with a ratio between 0.1 and 0.01, here). Therefore it would be desirable to resolve the contributions from both sides of a groove separately which could be done by contacting one cell of the module separately. This had not been done here in order to minimize the effect of disturbing heat wave reflections at the grooves and will be dealt with in a future publication.

ACKNOWLEDGMENT

This work was supported by the BMBF project SiThinSolar (contract no. 03IP607). The samples were kindly provided by CSG Solar AG, Thalheim.

REFERENCES

[1] O. Breitenstein, M. Langenkamp, *Lock-in Thermography*, Springer (2003)
[2] M. A. Green, P.A. Basore, N. Chang, D. Clugston, R. Egan, R. Evans, D. Hogg, S. Jarnason, M. Keevers, P. Lasswell, J. O'Sullivan, U. Schubert, A. Turner, S.R. Wenham, T. Young, Solar Energy 77 (2004) 857
[3] O. Breitenstein, R. Gupta, J. Schneider, Journal of Applied Physics 102 (2007) 024511/1-8
[4] H. Straube, J.-M. Wagner, O. Breitenstein, Applied Physics Letters 95 (2009) 052107
[5] G. S. Nolas, J. Sharp, H. J. Goldsmid, *Thermoelectrics*, Springer (2001)
[6] H. Straube, J.-M. Wagner, O. Breitenstein (to be published)